# ECS Transactions, 41 (4) 83-91 (2011) 10.1149/1.3628612 ©The Electrochemical Society

## Magnetically Modified Dye Sensitized Solar Cells

Garett G. W. Lee and Johna Leddv<sup>a\*</sup>

<sup>a</sup>Department of Chemistry, University of Iowa, Iowa City, IA 52242 \*johna-leddy@uiowa.edu

Magnetically modified, dye sensitized, n-type semiconductor electrodes were examined as a case study for magnetic field effects on electron transfer reactions in electrochemical power systems. Magnetic field effects arise through kinetics and mass transport; magnetic fields have negligible influence on system thermodynamics (i.e., no effects on open-circuit potential). Enhancements in the photocurrent response of dye sensitized TiO<sub>2</sub> semiconductor electrodes are observed.

#### Introduction

Revolutionized in the early 1990's by Michael Grätzel and coworkers, the dye-sensitized solar cell (DSSC), or Grätzel cell, is a second-generation, excitonic, photo-electrochemical device [1, 2]. Touted as an inexpensive alternative to traditional crystalline semiconductor-based photovoltaics (PV), DSSCs have received considerable attention over the last two decades. Research has focused on each area of the cell: the sensitizing dye [3-7], semiconductor film preparation [8-11], solid-state cells [12-17], photocathodes [18-20], and applications in areas such as water splitting [21-22]. The appeal of the DSSC lies in the combination of an amorphous, nanoparticulate semiconductor (e.g., TiO<sub>2</sub>), a photosensitive dye and regenerating redox couple that produces power densities similar to traditional single crystalline p-Si at significantly lower cost. To date, the best solar conversion efficiencies reported are 10.4% for DSSCs [23]. Before DSSCs can compete effectively with p-Si as viable solar cells, better efficiencies and high temperature stability coupled with high-turnover stability are needed.

Research at the University of Iowa has shown that magnetic fields affect electron transfer (ET) reactions in various power systems, including fuel cells and alkaline batteries [24, 25]. These effects have been demonstrated on homogeneous and heterogeneous ET reactions [26], for academically interesting redox probes (e.g., Ru(bpy)<sub>3</sub><sup>2+</sup>, tris(bipyridal) ruthenium(II)), as well as for absorbate reactions (e.g., for CO oxidation on platinum [24]). Magnetic fields affect current densities in power sources by altering the kinetics of ET. This modification method applied to DSSCs is a way to increase system efficiency.

Electronically, DSSCs are constrained by the standard reduction potential of the redox mediator and the Fermi level of the semiconductor. The most promising semiconductor to date is  $TiO_2$ , with an  $E_f$  = -0.5 V vs. SCE. It is commonly coupled with the iodine/iodide system in an organic solvent (e.g., acetonitrile, propylene carbonate) for the redox mediator ( $E^\circ$  = 0.4 V vs. SCE), restricting the maximum open-circuit potential ( $V_{oc}$ ) to 0.9V [2].

Here, the effect of magnetic fields on the electrochemistry of DSSCs is examined. Magnetic modification of the n-type DSSC occurs at the semiconductor electrode. DSSC electrodes are tested in a quartz photoelectrochemical cell in a two-electrode setup. Considerations of the magnetic materials used, magnetite (Fe<sub>3</sub>O<sub>4</sub>), neodymium iron borate (NdFeB), and samarium cobalt (SmCo<sub>5</sub>), included: particle size analysis, coatings, and film distribution. Particle loading percentages, magnetization protocol, and TiO<sub>2</sub> film preparation (i.e., annealing and pressing) were examined. In addition, preparation protocols based on film substrates were addressed.

Magnetically modified electrodes display average photocurrent enhancement compared to unmodified electrodes; an enhancement of 40% for magnetically modified electrodes is typically observed over a variety of loading percentages, magnetic materials and preparation methods. These current enhancements translate to increased power output over unmodified controls.

## **Experimental**

## Materials

All materials were used as received unless otherwise noted. Conductive substrates, coated with a transparent conductive oxide (TCO) of fluoride doped tin(IV) oxide, were purchased commercially. Polyethylene terephthalate (PET) substrates with resistivities of  $25\Omega/cm$  (SigmaAldrich) were cut into  $1in^2$  slides for use.

Two different commercial sources of  $TiO_2$  were used, nanoparticulate  $TiO_2$  (Aldrich), with average particle diameter of 25nm consisting primarily of anatase phase, and Aeroxide P25 (Acros), with a particle diameter of 21nm, consisting of a mixture of anatase and rutile crystal phases. The uses of each material are noted.

Electrodes were magnetically modified by adding eitherSmCo<sub>5</sub> (Alfa Aesar) and NdFeB (spherical annealed, Magnequench). Uncoated particles were primarily used. Coated magnetic particles are used in acidic electrochemical environments (e.g., Nafion® modified electrodes and PEM fuel cell membranes) to protect the particle from degradation and prevent the contamination of the electrochemical system from unwanted metal ions. In the studies presented herein, the nature of the environment and the timescale did not require coated particles. Ball-milled magnetite particles (Fe<sub>3</sub>O<sub>4</sub>, Chemalloy) were used in an SEM film analysis.

Principal components of the TiO<sub>2</sub> casting solsincluded Triton X100 (reduced, Sigma), acetyl acetone (Sigma), ethanol (200 proof, Decon Labs), and deionized water (DI). Iodine (Sigma), tetrafluoroborate iodide (Sigma), and acetonitrile (Fischer) stored over molecular sieves were used in the redox mediator solution. Ruthenizer 535 (N3) (Solaronix) molecular sensitizer was prepared in ethanol solutions.

#### Electrode Preparation

Unmodified casting sols contained TiO<sub>2</sub>, Triton X100, and acetyl acetone, in a mixture of DI and ethanol in equal proportions and a template was used to doctor-blade a 1cm<sup>2</sup> active area [1]. Electrodes prepared on PET substrates were annealed to 250°C for

two hours under vacuum, with an approximate ramp rate of 10°C/min. After cooling to room temperature, electrodes were equilibrated in a saturated solution of N3 dye in ethanol for at least 18 hours. No blocking layer or redox solutions additives were considered to optimize efficiency.

Electrodes were prepared as two layer electrodes. These two layer electrodes contain a single layer of unmodified  $TiO_2$  (annealed) on the ITO substrate. A second layer is bladed atop the first that contains 10% magnetic particles(by mass  $TiO_2$ ). Electrodes modified with  $SmCo_5$  are annealed under  $N_2(g)$  to prevent cobalt oxidation. Control electrodes were prepared similarly, two layer configurations without particles in the second layer (no difference in current behavior was observed between electrodes with two layers  $TiO_2$  versus one layer).

## **Analysis**

A twoelectrode configuration was used for all electrochemical analysis of the modified electrodes. A quartz cuvette with an optically flat window was used for photoelectrochemical measurements. A platinum mesh in a Teflon® housing served as the counter/reference electrode. A Teflon wedge was used to minimize the interelectrode distance (0.3mm). Approximately 1mL of the redox solution (0.5M TBAI and 0.04M  $I_2$  in acetonitrile) was added to the cuvette.

Electrochemical measurements were performed with a CH Instruments 760B potentiostat. The light source, an Oriel Solar Simulator with a 150W Xe-halogen lamp, was used in conjunction with an air mass (AM) 1.5 filter. Cyclic voltammetry was used for characterization. Lightpower measurements were taken with a ThorLabs D3MM Thermal Head sensor. Output from the solarsimulator is 20 mW/cm², the value used in efficiency calculations.

Particle and surface characterizations were accomplished by scanning electron microscopy (SEM, Hitachi S-3400N) complemented with elemental mapping. Elemental mapping was performed using a Bruker energy dispersive spectroscopy system - targeting iron and titanium.

#### **Results and Discussion**

## Surface and Particle Characterization

Particle and surface characterizations of the  $TiO_2$  films were undertaken to ensure maximum film homogeneity. Magnetically modified  $TiO_2$  electrodes were magnetized within an external magnetic field prior to annealing; to ensure that magnetic materials did not agglomerate during this procedure, samples were prepared analogously to the working electrodes, substituting an aluminum SEM sample stub for the PET substrate. Uncoated magnetite particles were ball milled in hexanes untilan average size of  $18.8 \pm 14.8 \mu m$  is reached. Particle distribution within annealed  $TiO_2$  is shown in Figures 1 and 2. Figure 3 is an SEM image of unmilled  $SmCo_5$  particles, which are of similar size and distribution to the magnetite particles analyzed.

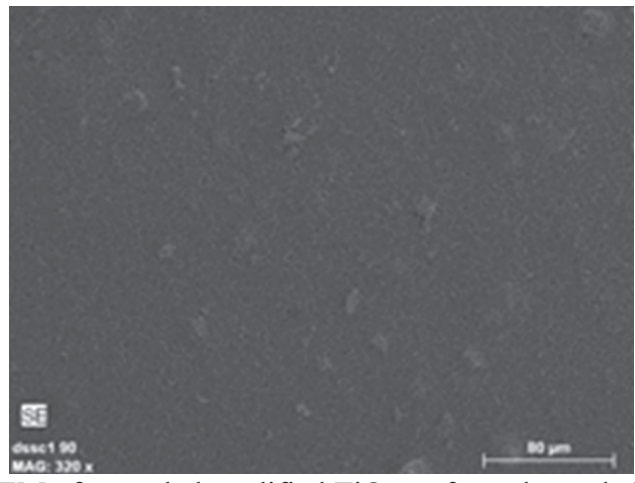
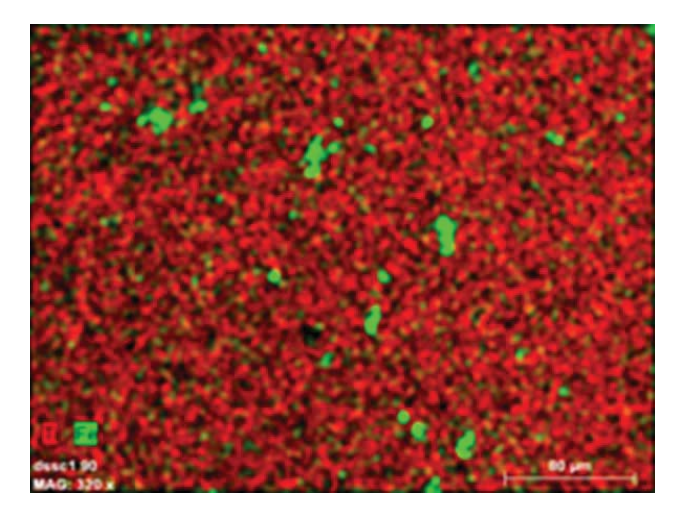
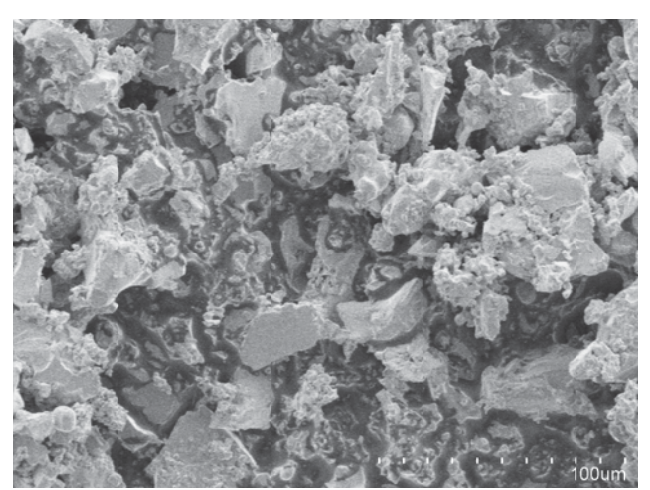


Figure 1. SEM of annealed modified TiO<sub>2</sub> surface; the scale bar is 80μm.



**Figure 2**. SEM of the same surface as in Figure 3, coupled with elemental mapping. Ti is falsely colored in red and Fe is falsely colored in yellow; the scale bar is 80μm.



**Figure3**. SEM of unmilled SmCo<sub>5</sub>, average particle size  $14.9 \pm 18.4 \mu m$  (n = 36).

## Electrochemical Measurements

Only electrochemical measurements from the first scans were recorded and analyzed. No long term measurements were conducted. Dye desorption into the redox solution was observed in voltammetric sweeps after the first scan. A dye desorption effect was observed over a series of electrode trials and measured by UV-vis of spent redox mediator solution. It has been shown that potentials greater than -1.0V vs. SCE encourage dye desorption [2] and this, in addition to the relatively large volume of redox solution used to make the measurements, may have further induced dye desorption.

Although electrodes were prepared by a variety of methods, utilizing different materials and structures, this article focuses on PET substrates. Variation in data due to the magnetic material was observed.

## **Energy Conversion Efficiency Calculation**

Precise measurements of open-circuit potential  $(V_{oc})$ , short-circuit current density $(J_{sc})$ , and input power $(W_{in})$  are important for calculating fill factor (FF) and photovoltaic efficiency. Fill factor and efficiency calculation were used as criteria for evaluating the enhancement of modified cells over unmodified cells. Fill factor is defined as:

$$FF = \frac{J_{mp}V_{mp}}{V_{oc}J_{sc}}$$
 [1]

where  $J_{mp}$  and  $V_{mp}$  are current density and voltage at maximum power, respectively.  $J_{mp}$  and  $V_{mp}$  are determined from a power curve (potential versus power). Photovoltaic efficiency is defined as:

$$n = \frac{(V_{mp}J_{mp})}{W_{in}} \times 100$$
 [2]

where  $W_{in} = 20 \text{mW/cm}^2$ .

#### PET Substrate-based Electrodes

The upper limit for annealing PET based electrodes is restricted to the melting point of PET (~ 250 °C). At 250 °C,  $TiO_2$  films achieve stability for electrochemical analysis. Electrodes prepared on PET were annealed at 250°C for 2 hours. When modified with  $SmCo_5$ , annealing occurred under vacuum (~900 mTorr). Vacuum prevents the oxidation of  $SmCo_5$  modified electrodes. Advantageously, 250°C is below the Curie temperature ( $T_c$ ) of NdFeB.  $T_c$  is the temperature above which a magnetis demagnetized ( $T_c$  for NdFeB ~ 300 °C,  $T_c$  for  $SmCo_5 \sim 800$ °C).

Both SmCo<sub>5</sub> and NdFeB modified electrodes display enhanced currentresponses versus unmodified control electrodes. Figure 4 shows an iV-curve for NdFeB modified electrodes vs. unmodified electrodes. NdFeB modified electrodes display the greatest photocurrent ( $i_{ph}$ ) enhancement. This is not unexpected, as magnetic effects are proportional to a material's magnetic energy product, measured in MegaGauss-oerstads (MGo). The maximum energy product of NdFeB is almost twice that of SmCo<sub>5</sub> magnets (12-24 MGo for SmCo vs. 18-48MGo for NdFeB) [26]. Figure 5 shows the  $i_{ph}$  response of SmCo<sub>5</sub> modified electrodes on PET. Table I gives average efficiency values (based on equation 2) and statistics for the electrodes displayed in Figures 4 and 5. Magnetic effects on fill factor values are negligible (< 0.2%); these values are not tabulated.

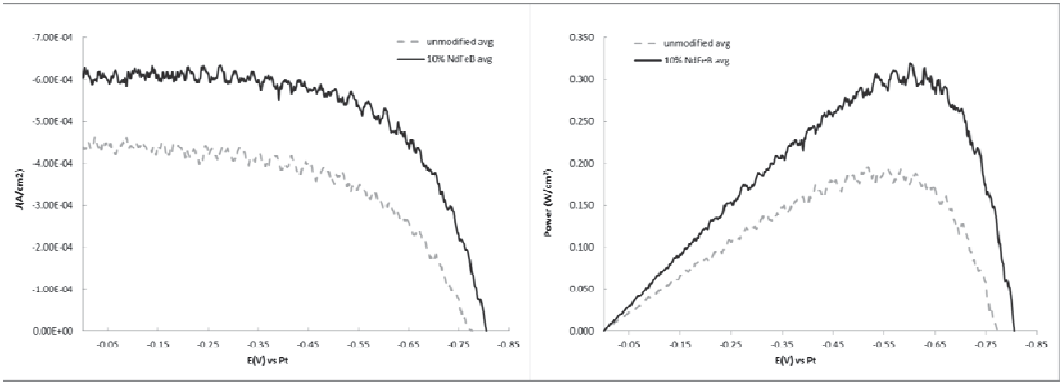


**Figure 4**. iV-curve of 10% NdFeB modified electrodes versus unmodified electrodes on PET substrates, average  $i_{ph}$  response for n = 2 electrodes of each loading.

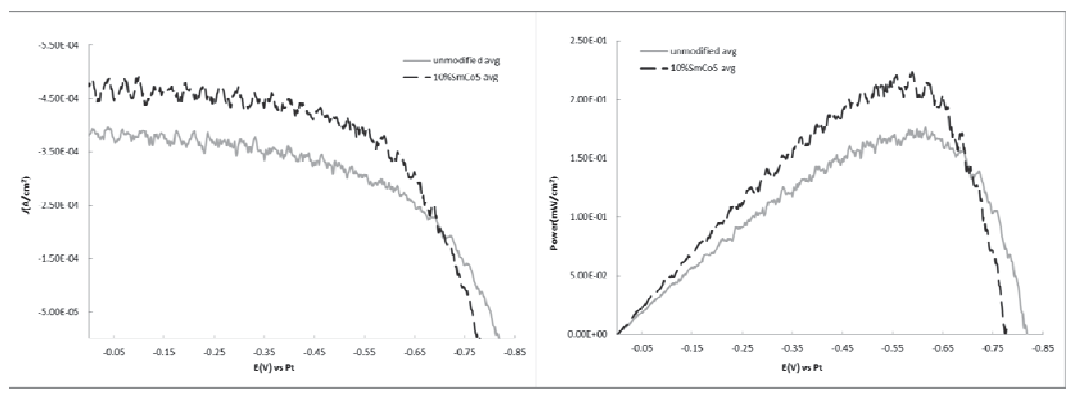


**Figure 5**. iV-curve of 10% SmCo<sub>5</sub> modified electrodes versus unmodified electrodes on PET substrates, average  $i_{ph}$  response for n = 2 electrodes of each loading.

**TABLE I.** Efficiency calculations of electrodes on PET substrate (vs. platinum reference).

Modification	V <sub>oc</sub> (V vs. Pt)	$J_{sc}$ (mA/cm <sup>2</sup> )	Average Efficiency (%)	Max. Power (mW/cm <sup>2</sup> )
Unmodified blank	-0.770 (± 2.9%)	-0.438 (± 18.5%)	0.98%	0.20
10% NdFeB	-0.806 (± 3.7%)	-0.606 (± 10%)	1.59%	0.32
Unmodified blank	-0.818 (± 1.6%)	-0.383 (± 6.1%)	0.88%	0.18
10% SmCo <sub>5</sub>	$-0.783~(\pm~0.25\%)$	$-0.473~(\pm~5.8\%)$	1.22%	0.22

The  $i_{\rm ph}$  response of NdFeB modified electrodes returns Student's t values that are significantly different than the control electrodes at a 90% confidence interval. The  $i_{\rm ph}$  response of SmCo<sub>5</sub> modified electrodes returns Student's t values that are significantly different than the control electrodes at a 90% confidence interval. NdFeB modified electrodes show an average relative efficiency increase of 62% over unmodified electrodes. SmCo<sub>5</sub> modified electrodes show an average increase of 39% over unmodified controls.

## Analysis of Magnetic Effects on ET Reactions in DSSC

Figure 8 is a standard, accepted representation of a dye-sensitized solar cell system under operation.

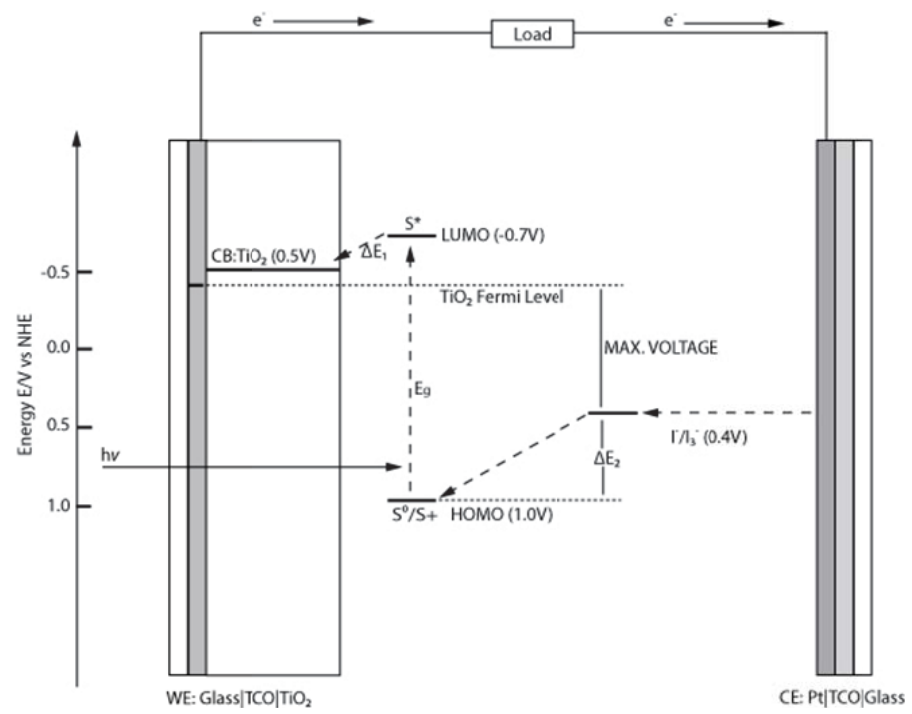


Figure 6. DSSC schematic [23]

Multiple steps and electron transfer reactions are required to complete the cell and generate power.

- 1. Incident light (photons) excites a sensitizing dye (S), traditionally a transition metal complex, to an excited state (S\*).
- 2. The excited dye transfers an electron to the conduction band (CB) of the semiconductor (SC), traditionally  $TiO_2$ , at  $ET_1$ .
- 3. The electron diffuses through the SC to a transparent conductive oxide (TCO) and onto the external load; this step is realized as power.
- 4. To complete the circuit, electrons reduce a sacrificial donor, D to D<sup>-</sup>, via ET<sub>2</sub>.
- 5. The sacrificial donor then reduces the dye  $S^*$  back to S in  $ET_3$ , which allows the cycle to repeat.

Of fundamental importance is the mechanism by which magnetic modification increases the  $i_{\rm ph}$  response. Three ET reactions are realized in a functioning DSSC: a heterogeneous exciton ET at the dye|semiconductor interface, a homogeneous ET reaction between the dye and the redox mediator, and a second heterogeneous ET reaction between the counter electrode (CE) and the redox mediator.

Modification occurs at the semiconductor working electrode. Given the distance between the CE and the magnetic microparticles, ET<sub>3</sub> is most likely unaffected. For example, magnetic field strengths at spherical particles decrease with particle radius r<sup>-3</sup> [26]. At distances greater than 5 radii, field effects are negligible.

It is established that magnetic microparticles increase current response in self-exchange reactions [26]. Additionally, heterogeneous ET transfer rates are increased at modified electrodes. This enhanced current response can be seen for Ru(bpy)<sub>3</sub><sup>2+</sup> at modified glassy carbon electrodes in Figure 7. The ruthenium dye complex N3 (*cis*-bis(isothiocyanato)bis(2,2'-bipyridyl-4,4'-dicarboxylato)-ruthenium(II)) is an analogous

ruthenium-bipyridine complex to  $\text{Ru(bpy)}_3^{2^+}$ . An enhancement in the ET rate from the excited N3 dye to the conduction band of  $\text{TiO}_2$  at  $\text{ET}_1$  is a possible reason for  $i_{\text{ph}}$ -response enhancement.

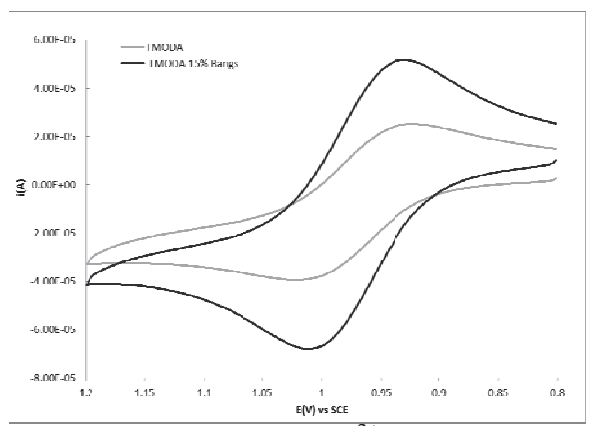


**Figure 7.** Cyclic voltammagram of Ru(bpy)<sub>3</sub><sup>2+</sup> at trimethyloctadecyl ammonium (TMODA) Nafion® modified glassy carbon (GC) electrodes; TMODA modified control electrodes and 15% (by vol TMODA film) Bangs<sup>TM</sup> coated-magnetite (Fe<sub>3</sub>O<sub>4</sub>).

Cross-exchange rates are also affected by magnetic fields [24-27]. Transition state theory is proposed to account for this. At high concentrations, when diffusion by hopping is prominent, magnetic fields have been shown to increase self-exchange rates. At  $ET_2$ , the electron is transferred between the redox mediator and the ground state dye (S°). Estimates of the oxidized dye and the redox mediator ( $\Gamma$ ) interception are on the order of microseconds [2]. Thus, an increase in the regeneration turnover rate may also account for the observed enhancement.

#### **Summary**

Magnetically modified, dye sensitized, n-type semiconductor electrodes display enhanced photocurrent response versus unmodified control electrodes. Modification takes place in the semiconductor layer, and is thought to effect the system through kinetics (e.g., enhanced photocurrent) and not thermodynamics. That is, magnetic fields should not be affecting the photoinduced chemical potential gradients that are currently thought to be responsible for photovoltage determination [28]. Considerations were given to fabrication and magnetic materials. Continued efforts are focused on understanding the mechanism and the effects of magnetic materials on the system.

#### Acknowledgments

Support of the NSF and The University of Iowa for this project is acknowledged gratefully.

#### References

- 1. O'Regan, B.; Grätzel, M. *Nature*. **353**, 737-740 (1991).
- 2. Hagfeldt, A.; Boschloo, G.; Sun, L.; Kloo, L.; Pettersson, H. *Chem. Rev.* 100, 6595-6663 (2010).

- 3. Stergiopoulos, T.; Karakostas, S.; Falaras, P. *J. Photochem. Photobio.***162**, 331-340 (2004).
- 4. Cazzanti, S.; Caramori, S.; Argazzi, R.; Elliot, C. M.; Bignozzi, C. A. *J. Am. Chem. Soc.* **128**, 9996-9997 (2006).
- 5. Yanagide, M.; Yamaguchi, T.; Kurashige, M.; Hara, K.; Katoh, R.; Sugihara, H.; Arakawa, H. *Inorg. Chem.***42**, 24 (2003).
- 6. Hasobe, T.; Hattori, S.; Kamat, P.; Urano, Y.; Umezawa, N.; Nagano, T.; Fukuzumi, S. *Chem. Phys.***319**, 243-252 (2005).
- 7. Ismail, Y.; Soga, T.; Jimbo, S. Sol. Energy Mater. Sol. Cells 93, 1582-1586 (2009)
- 8. Chi, C.; Liau, S.; Lee, Y. Nanotech. 21, 025202 (2010).
- 9. Hossain, M.; Biswas, S.; Shahjahan, M.; Majumder, A.; Takahashi, T. *J. Vac. Sci. Technol. A.* **27**, 4 (2009).
- 10. Brooks, K.; Burnside, S.; Shklover, V.; Comte, P.; Arendse, F.; McEvoy, A.; Grätzel, M. *Electrochem. Mater. Devices.* 115-121 (1999).
- 11. Lindström, H.; Boschloo, G.; Lindquist, S.; Hagfeldt, A. *ACS Symposium Series*. **2003**, ACS, Washington D.C. (Pressed)
- 12. Kim, J. Kang, M.; Kim, Y.; Won, J.; Park, N.; Kang, Y. *Chem. Commun*. 1662-1663 (2004).
- 13. Singh, P.; Bhattacharya, B.; Nagarale, R.; Kim, K.; Rhee, H. *Syn. Mater.* **160**, 139-143 (2010).
- 14. Buraidah, M.; Teo, L.; Majid, S.; Arof, A. Optical Mater. 32, 723-728 (2010).
- 15. Buraidah, M.; Teo, L.; Majid, S.; Yahya, R.; Taha, R.; Arof, A. *Int. J. Photoenergy.* 805836 (2010).
- 16. Katsaros, G.; Stergiopoulos, T.; Arabatzis, I.; Papadokostaki, K.; Falaras, P. *J. Photochem. Photobio.***149**, 191-198 (2002).
- 17. Bai, Y.; Cao, Y.; Zhang, J.; Wang, M.; Li, R.; Wang, P.; Zakeeruddin, S.; Grätzel, M. *Nature Mater.* **7**, 626-630 (2008).
- 18. Odobel, F.; Pleux, L.; Pellegrin, Y.; Blart, E. *Acct. Chem. Res.* **43**, 1063-1071 (2010).
- 19. Nattestad, A.; Ferguson, M.; Kerr, R.; Cheng, Y.; Bach, U. *Nanotechnology*. **19**, 295304 (2008).
- 20. Mizoguchi, Y.; Fujihara, S. *Electrochem. Solid-State Letters.***11**, K78-K80 (2008).
- 21. Caramori, S.; Cristino, V.; Argazzi, R.; Meda, L.; Bignozzi, C. *Inorg. Chem.* **49**, 3320-3328 (2010).
- 22. Youngblood, W.; Lee, S.; Maeda, K.; Mallouk, T. Acct. Chem. Res. 42, 1966-1973 (2009).
- 23. Semiconductor Photochemistry and Photophysics. Molecular and Supermolecular Photochemistry. Vol. 10. Ed. V. Ramamurthy and K. S. Schanze. Marcel Dekker, Inc. New York, 2003.
- 24. Gellett, W. L. Ph. D. Thesis, The University of Iowa, 2004.
- 25. Dunwoody, D. C. Ph. D. Thesis, The University of Iowa, 2003.
- 26. Tesene, J. P. Master's Thesis, The University of Iowa, 2005.
- 27. Lee, H. C. Ph. D. Thesis, The University of Iowa, **2010**.
- 28. Pichot, F.; Gregg, B. J. Phys. Chem. B.104, 6-10 (2000).